Supporting Information

Implantable hydrogel embedded dark-gold nanoswitch as a theranostics probe to sense and overcome cancer multidrug resistance

João Conde [1,2,*], Nuria Oliva[1] and Natalie Artzi[1,3,*]

[1] Institute for Medical Engineering and Science, Massachusetts Institute of Technology (MIT), Cambridge, MA 02139, USA.

[2] School of Engineering and Materials Science, Queen Mary University of London, London E1 4NS, UK.

[3] Department of Anesthesiology, Brigham and Women's Hospital, Harvard Medical School, Boston, Massachusetts 02115, USA.

* Corresponding authors. Natalie Artzi, nartzi@mit.edu and João Conde, jdconde@mit.edu

Keywords: hydrogels; gold nanobeacons; theranostics; breast cancer; multidrug resistance.

S1. Functionalization and characterization of gold nanoparticles (AuNPs)

S1.1. Functionalization of AuNPs with poly(ethylene glycol) (PEG)

Briefly, 10 nM of bare AuNPs dispersed in aqueous solution of 0.01×PBS (Cytodiagnostics) were mixed with 0.006 mg/mL of a commercial hetero-functional (PEG α-Mercapto-ω-carboxy PEG solution, HS-C_2H_4-CONH-PEG-O-C_3H_6-COOH, MW. 3500 Da, Sigma) in an aqueous solution of SDS (0.08%). PEG excess was removed by centrifugation (20.000 ×g, 30 min, 4 ºC) and quantified by the Ellman's Assay as described elsewhere [S1,S2]. The excess of thiolated chains in the supernatant was quantified by interpolating a calibration curve set by reacting 200 μL of α-Mercapto-ω-carboxy PEG solution in 100 μL of phosphate buffer (0.5 M, pH 7) with 7 μL 5,5'-dithio-bis(2-nitrobenzoic) acid (DTNB, 5 mg/mL) in phosphate buffer (0.5 M, pH 7) and measuring the absorbance at 412 nm (**Figure S1A**) after 10 minutes reaction. The linear range for the PEG chain (**Figure S1B**) obtained by this method is 0–0.1 mg/mL (Abs at 412nm = 6.8991×[PEG, mg/mL] + 0.0588). The number of exchanged chains is given by the difference between the amount determined by this assay and the initial amount incubated with the AuNPs. There is a point at which the nanoparticle becomes saturated with a thiolated layer and is not able to take up more thiolated chains - maximum coverage per gold nanoparticle, i.e. 0.02 mg/mL of PEG (**Figure S1C**). The AuNPs were functionalized with 0.006 mg/mL of PEG corresponding to 30% of PEG saturation on nanoparticle's surface (168.32 ± 2.19 PEG chains per nanoparticle). Stability of AuNPs with increasing PEG concentration was evaluated by measuring the ratio of absorbance 520/600 nm, measuring the ratio between non-aggregated and aggregated NPs [S3,S4]. A maximum stability was achieved upon functionalization with 0.02 mg/mL of PEG (**Figure S1D**), validating the results for PEG saturation in **Figure S1C**.

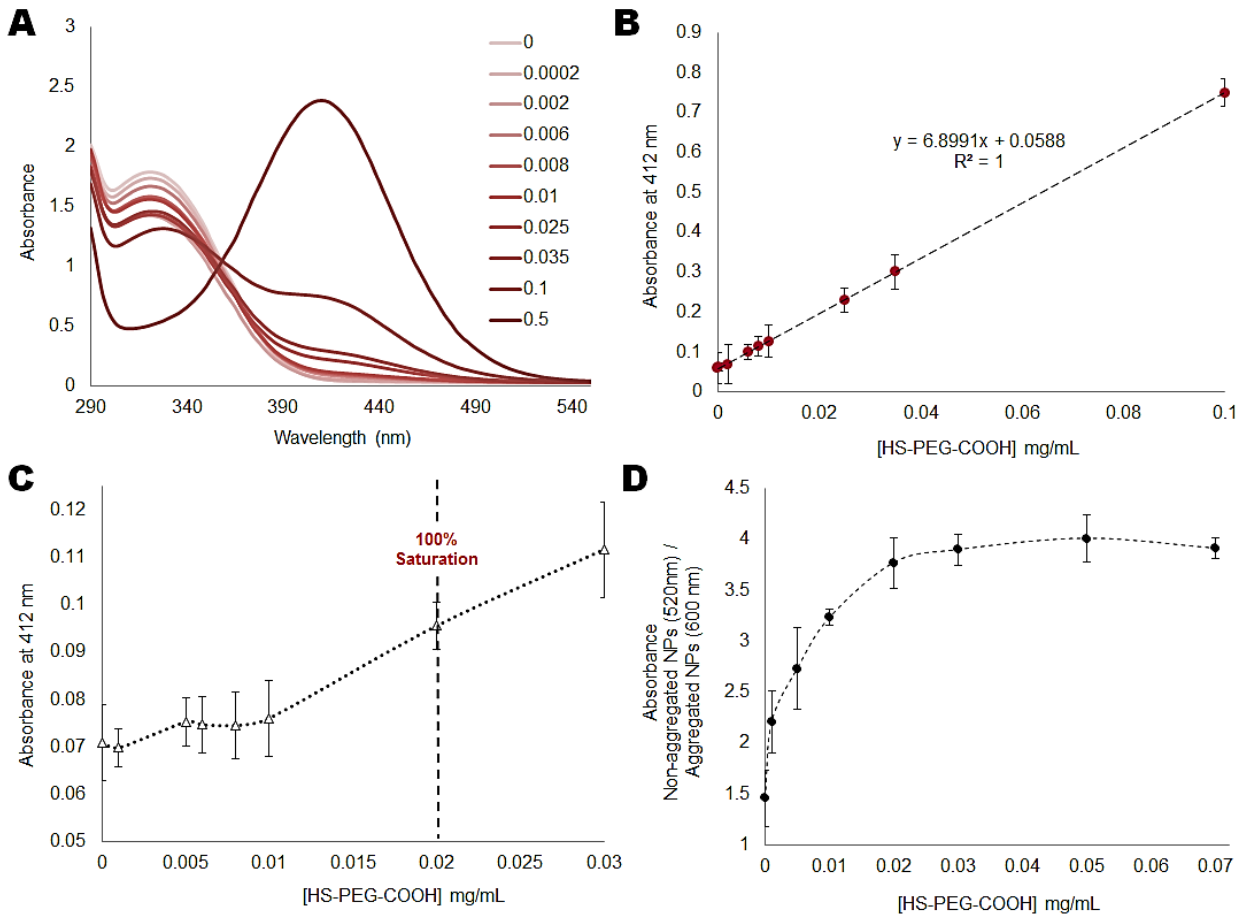

Figure S1. (**A**) Absorbance spectra of DTNB after reaction with increasing amounts (0–0.1 mg/mL) of thiolated PEG. (**B**) Standard calibration curve for PEG chains, whose concentration can be calculated via the following equation: Abs at 412nm = 6.8991×[PEG, mg/mL] + 0.0588, R^2=1. (**C**) Variation of the excess of PEG thiolated chains as a function of the initial concentration in the incubation with 10 nM of AuNPs. The dashed vertical line indicates the 100% saturation, i.e. the PEG concentration above which no more PEG can be bound to the nanoparticle's surface. (**D**) Ratio between non-aggregated (at 520 nm) and aggregated NPs (at 600 nm) after functionalization with increasing amounts (0–0.07 mg/mL) of thiolated PEG.

S2. Quantification of beacon coverage on AuNP@PEG

Coverage, i.e. average number of labeled beacons per nanoparticle was assessed by the quantification of the excess of the thiolated oligonucleotides (beacons) from the gold nanobeacon synthesis. Oligomers sequences are depicted in **Table S1.** All the three supernatants containing the unbound

oligonucleotides were measured by monitoring the emission spectra of Quasar 705 (Exc = 675 nm) dye in a microplate reader (Varioskan Flash Multimode Reader, Thermo Scientific). All the AuNPs samples and the standard solutions of the thiol-oligonucleotide beacon were kept at the same pH and ionic strength and calibration for all measurements. Fluorescence emission was converted to molar concentrations of the thiol modified oligonucleotide by interpolation from a standard linear calibration curve. Standard curves were prepared with known concentrations of beacon using the same buffer pH and salt concentrations. The average number of molecular beacon strands per particle was obtained by dividing the oligonucleotide molar concentration by the AuNP concentration.

The total number of thiolated-beacon chains that can be attached per gold nanoparticle are depicted in **Table S2.**

Table S1. Oligomers sequences used in dark-gold nanobeacons assembly.

Oligomers	**Sequence and modifications**
nanobeacon anti-MRP1	Thiol- 5'tttgcatGGCTACATTCAGATGACACatgcaaa 3' -Q705
nanobeacon anti-Luc	Thiol- 5' tttgcatCGTACGCGGAATACTTCGAatgcaaa 3' -Q705
nanobeacon nonsense	Thiol- 5' tttgcatTTCTCCGAACGTGTCACGTatgcaaa 3'-Q705
Oligo-BHQ2 dark quencher	Thiol- 5' TTTGGG 3' -BHQ2
MRP1 target	5'-GTGTCATCTGAATGTAGCC-3'

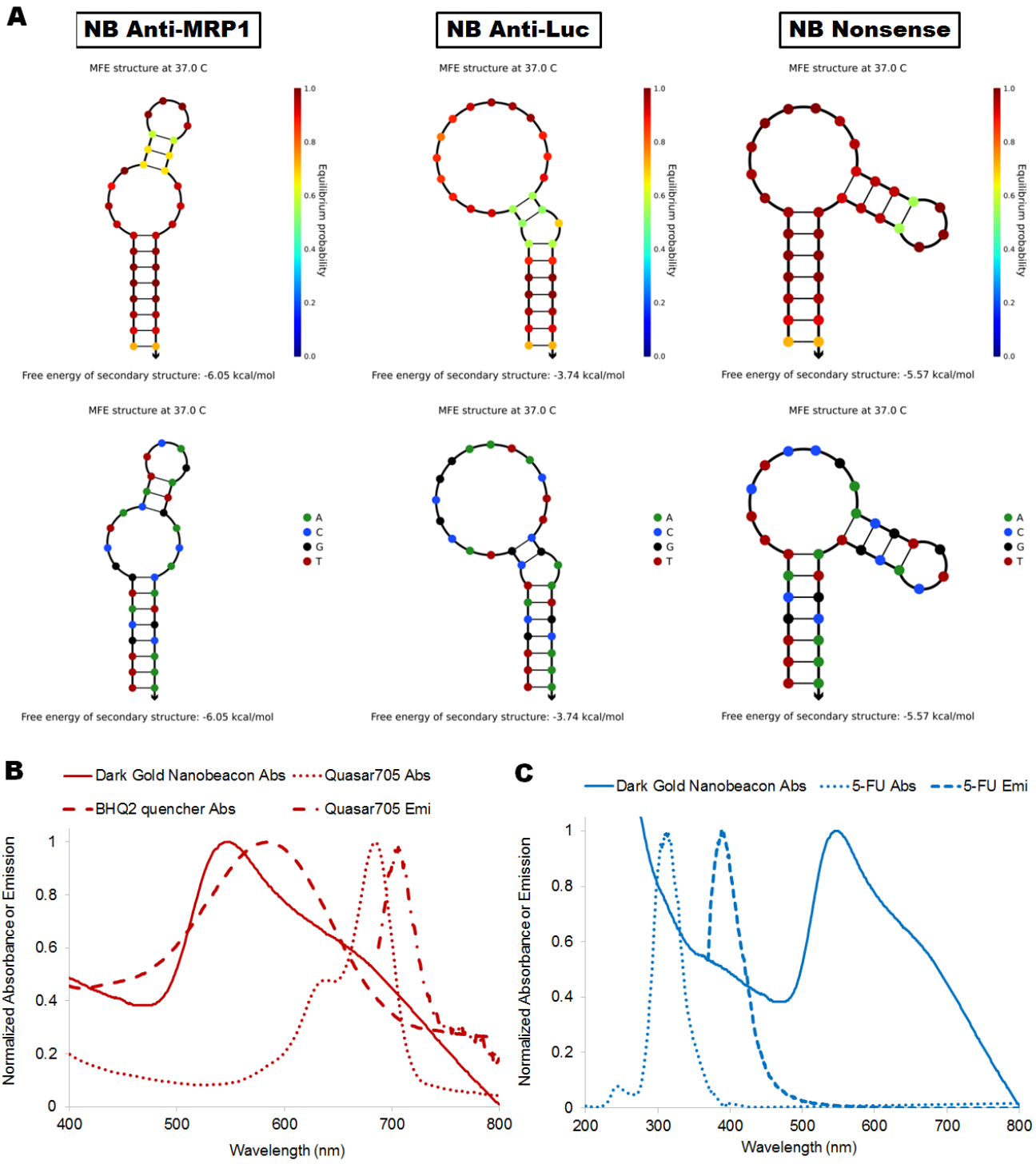

Figure S2. (A) Two-dimensional structures of the sequences for nanobeacons anti-MRP1, anti-Luc and nonsense at 37ºC, as predicted by NUPACK [S5]. (**B**) Normalized absorbance and emission spectra of dark-gold nanobeacon (gold nanoparticles functionalized with DNA oligo with BHQ2 dark quencher), free DNA oligo labeled with Q705 and free DNA oligo with BHQ2 dark quencher. (**C**) Normalized absorbance and emission spectra of gold nanobeacon (gold nanoparticles functionalized with DNA oligo labeled with Q705) and free drug 5-FU.

Table S2. Physico-chemical properties of Dark-gold nanobeacons.					
Dark-gold nanobeacons	**SPR peak**	**Size (nm)** [a]	**Hairpin-Q705 mol per particle**	**Oligo-BHQ2 mol per particle**	**5-FU mol per particle**
nanobeacon anti-MRP1	548	25.6 ± 1.4	28.6 ± 5.1	27.4 ± 4.8	NA
nanobeacon anti-Luc	548	25.1 ± 1.3	29.4 ± 3.7	27.7 ± 1.9	NA
nanobeacon nonsense	548	25.8 ± 0.8	28.1 ± 3.9	26.9 ± 4.5	NA
nanobeacon anti-MRP1 + 5-FU	550	30.9 ± 0.5	28.6 ± 5.1	23.4 ± 4.8	98.4 ± 6.7
nanobeacon anti-Luc + 5-FU	550	31.2 ± 0.7	29.4 ± 3.7	22.7 ± 1.9	101.2 ± 8.6
nanobeacon nonsense + 5-FU	550	31.0 ± 0.4	28.1 ± 3.9	23.9 ± 4.5	99.3 ± 8.2

[a] Determined by Dynamic Light Scattering (DLS).

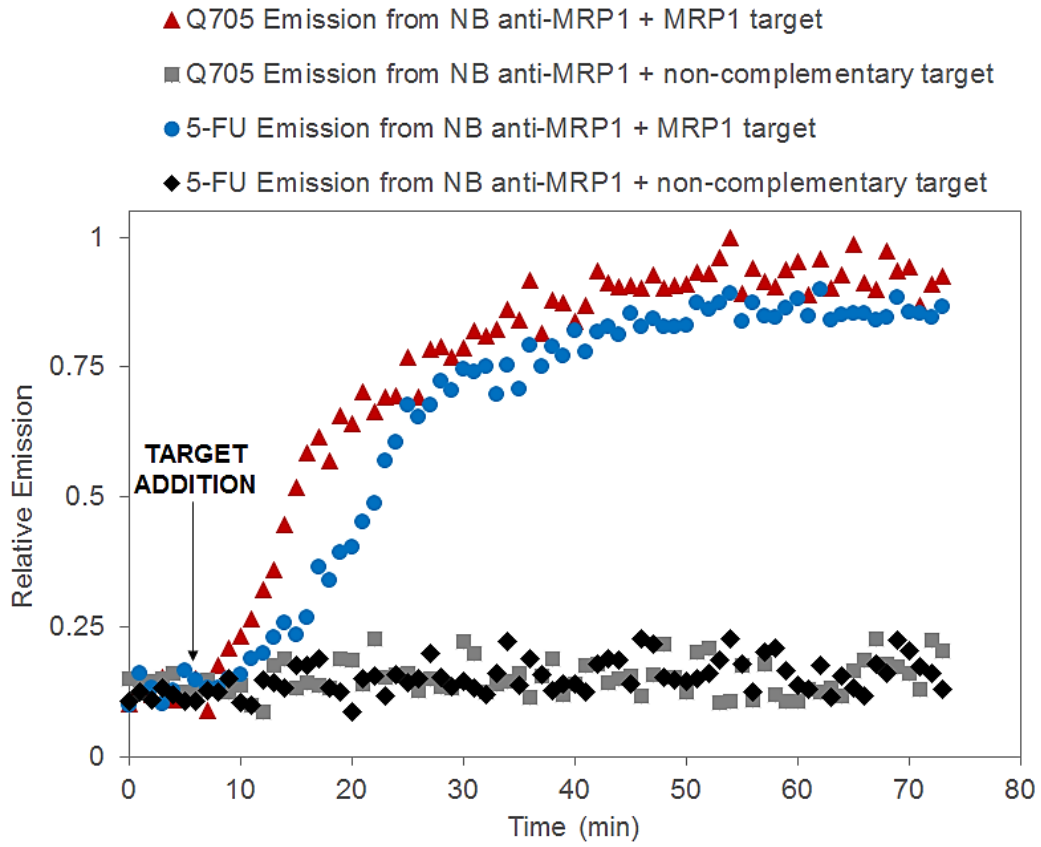

Figure S3. Kinetics of the release of the drug intercalated in the nanobeacons, the fluorescence of the 5-FU (Emission at 400 nm) was measured during 75 minutes following addition of 1 µM of target (at 5 minutes of incubation) and compared to the fluorescence of the Q705 (Emission at 705 nm).

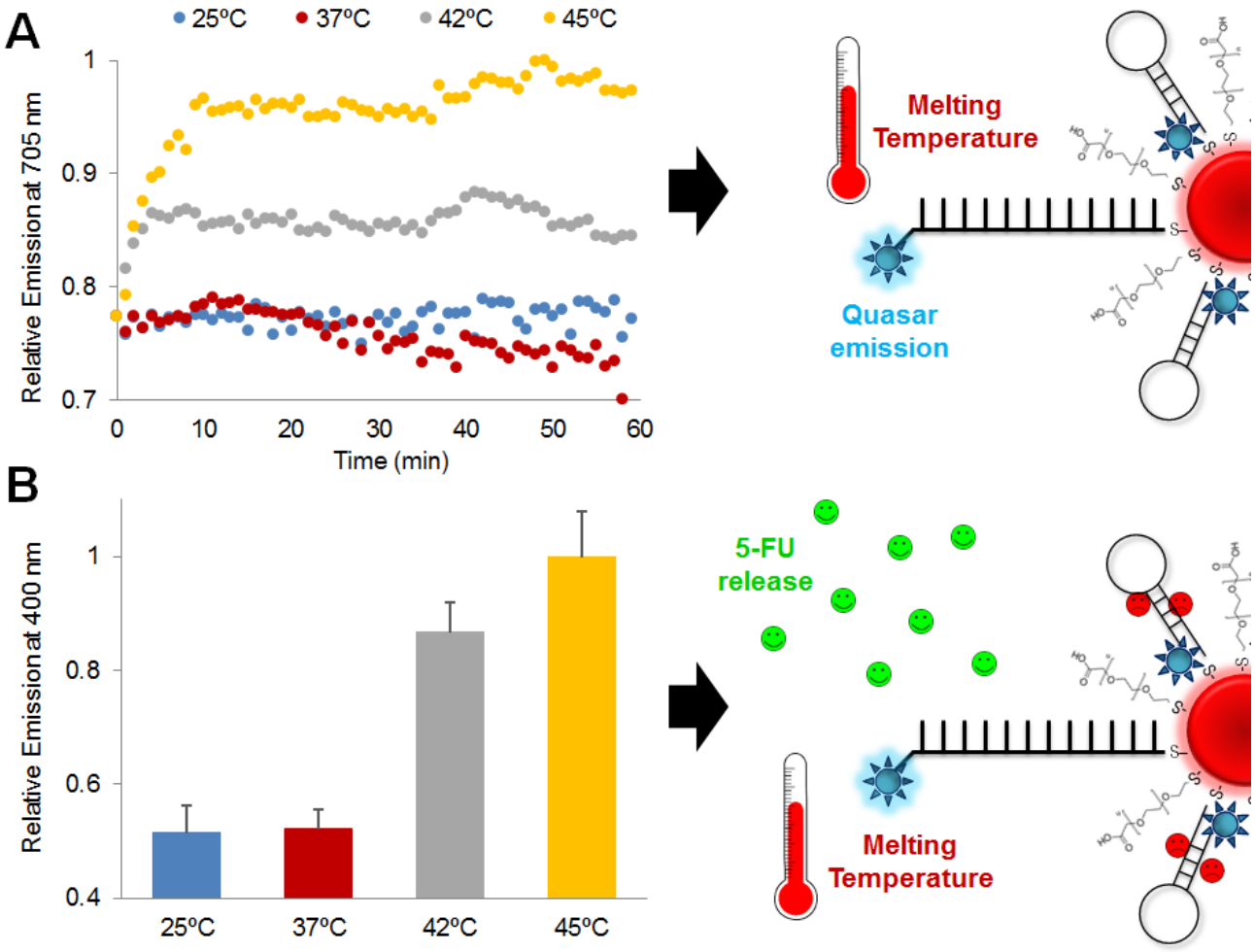

Figure S4. Effect of temperature on nanobeacon signal and 5-FU release. (**A**) Stability of dark-gold nanobeacon loaded with 5-FU towards variations with temperature (25, 37, 42 and 45ºC) over time. (**B**) Drug (5-FU) release profile with temperature.

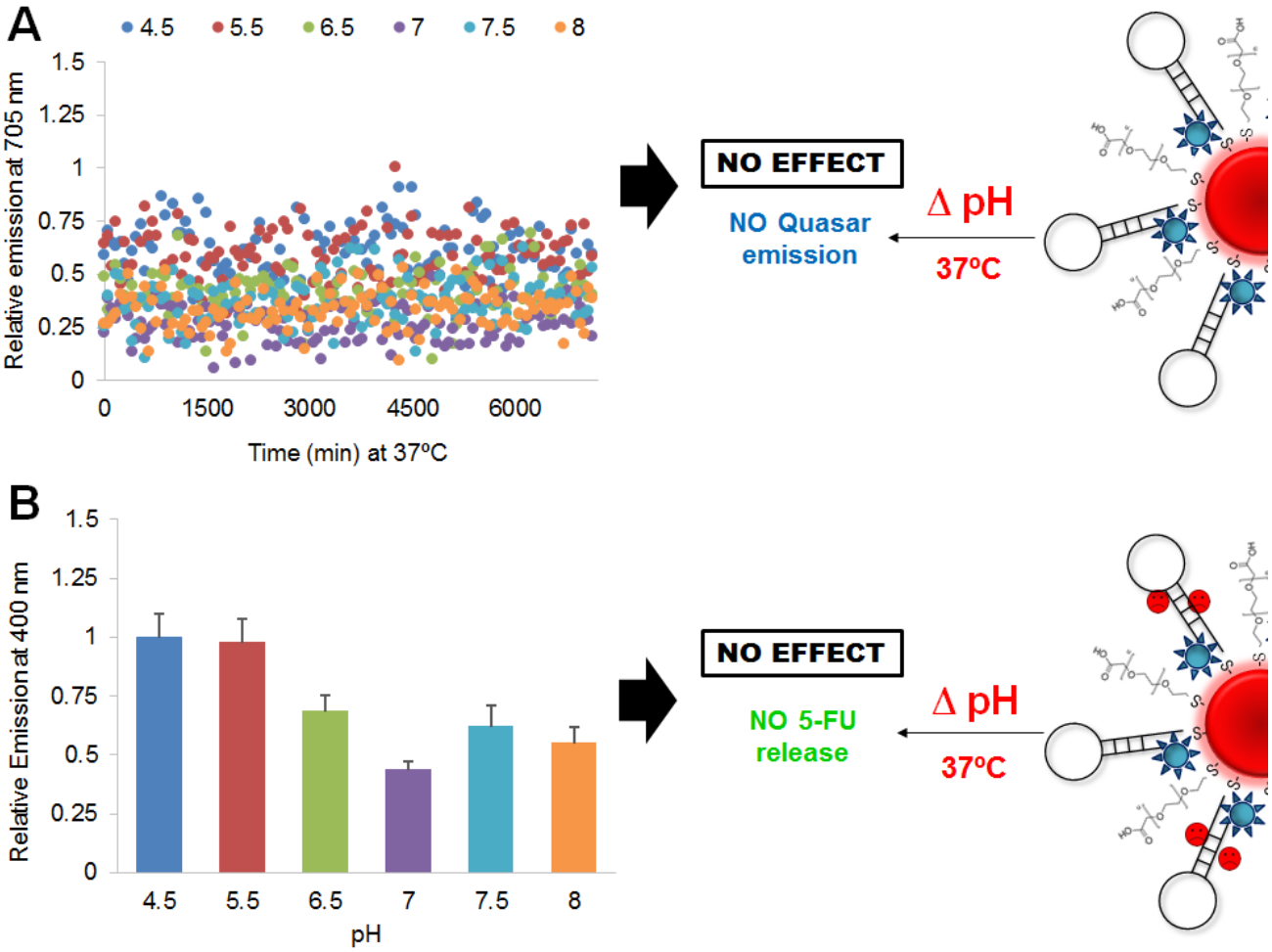

Figure S5. Effect of pH on nanobeacon signal and 5-FU release. (**A**) Stability of dark-gold nanobeacon loaded with 5-FU towards variations with a wide pH range (4.5 to 8) over time at 37ºC. (**B**) Drug (5-FU) release profile at different pHs.

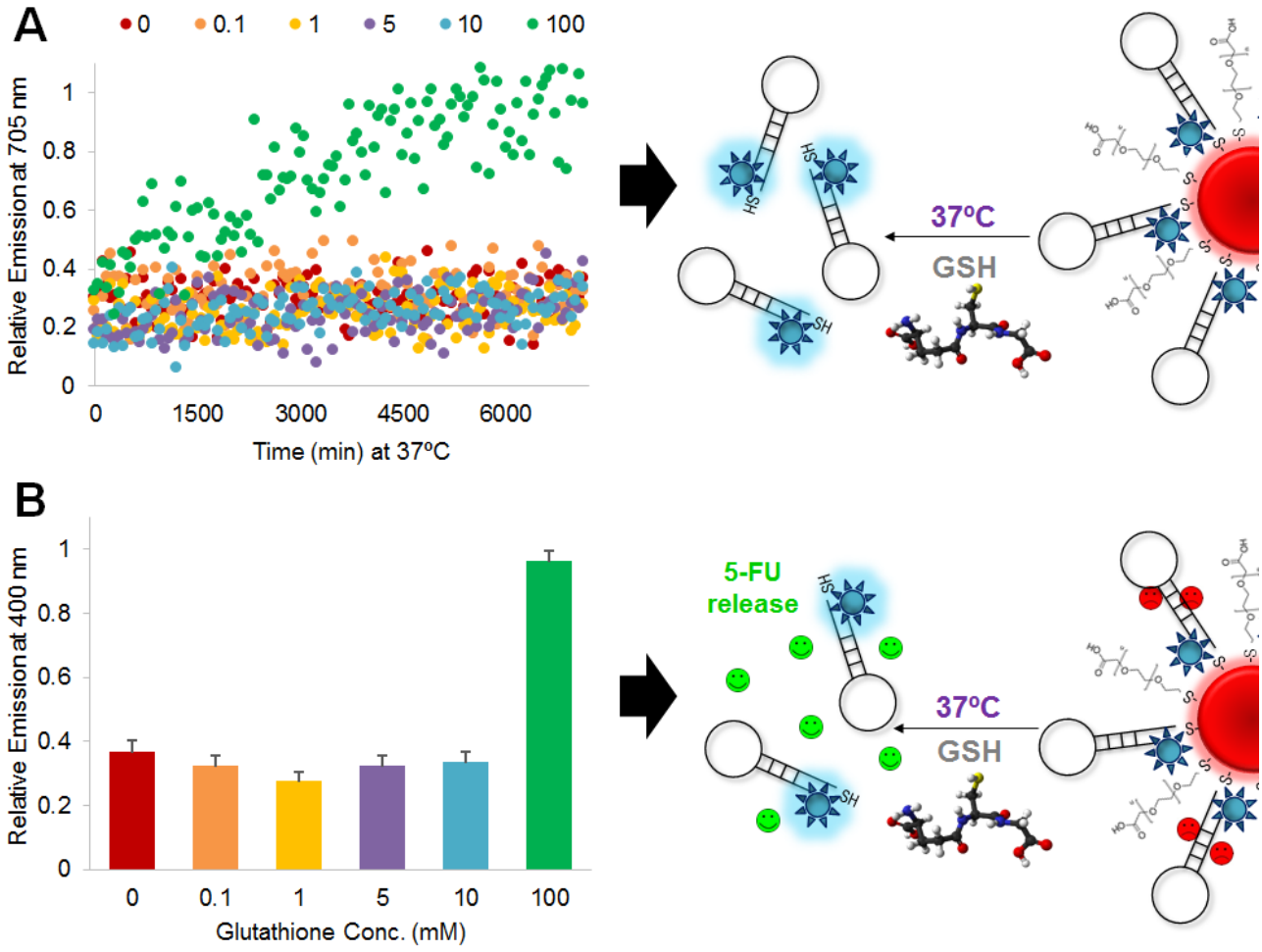

Figure S6. Effect of glutathione (GSH) concentration on nanobeacon signal and 5-FU release. (**A**) Stability of dark-gold nanobeacon loaded with 5-FU towards increase concentrations of glutathione (0.1, 1, 5 - physiological concentration, 10 and 100 mM) over time at 37ºC. (**B**) Drug (5-FU) release profile at different glutathione concentrations.

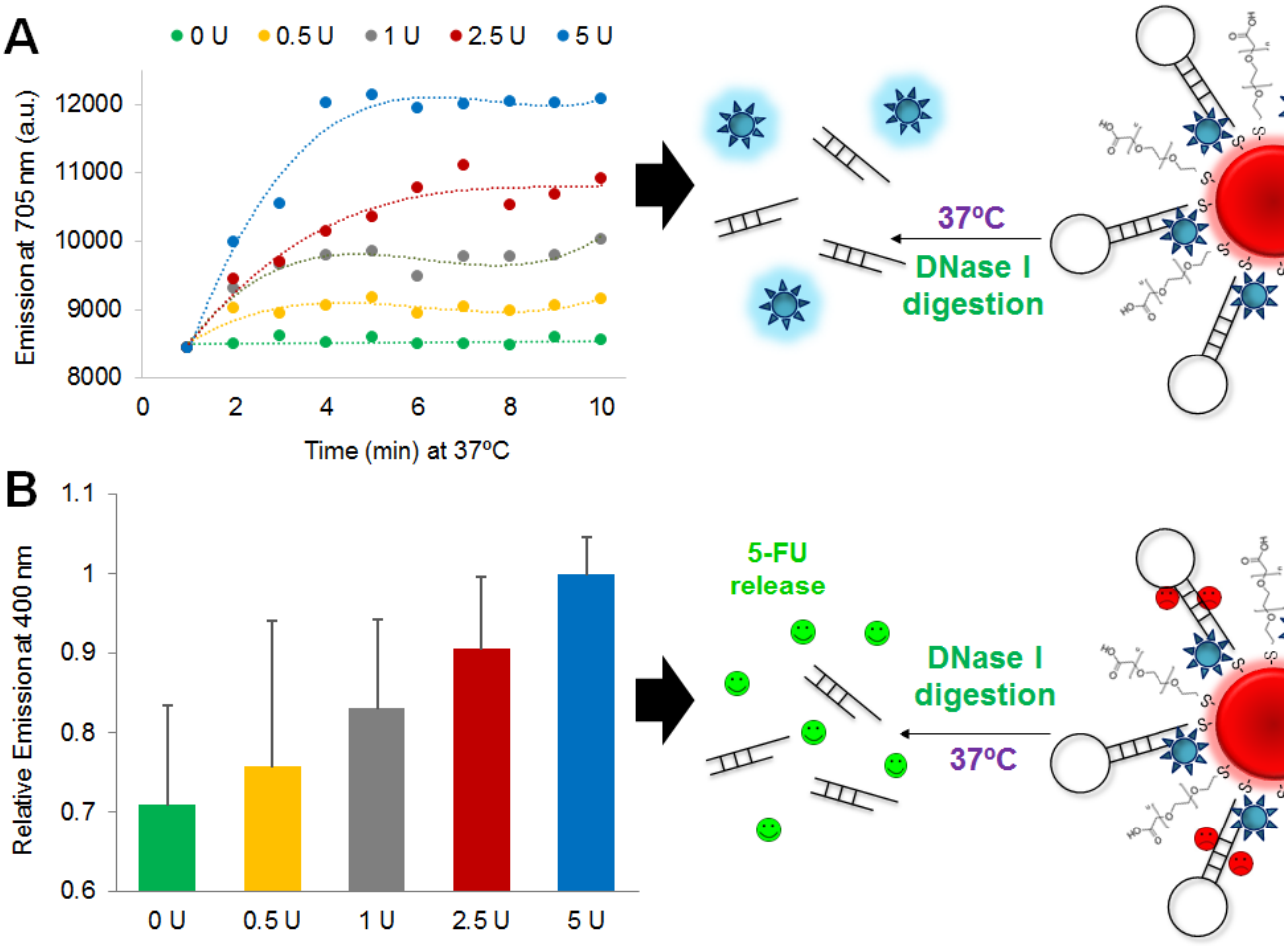

Figure S7. Effect of DNase I concentration on nanobeacon signal and 5-FU release. (**A**) Stability of dark-gold nanobeacon loaded with 5-FU towards increase concentrations of DNase I (0.5, 1, 2.5 and 5 Units) over time at 37ºC. (**B**) Drug (5-FU) release profile at different DNase I concentrations.

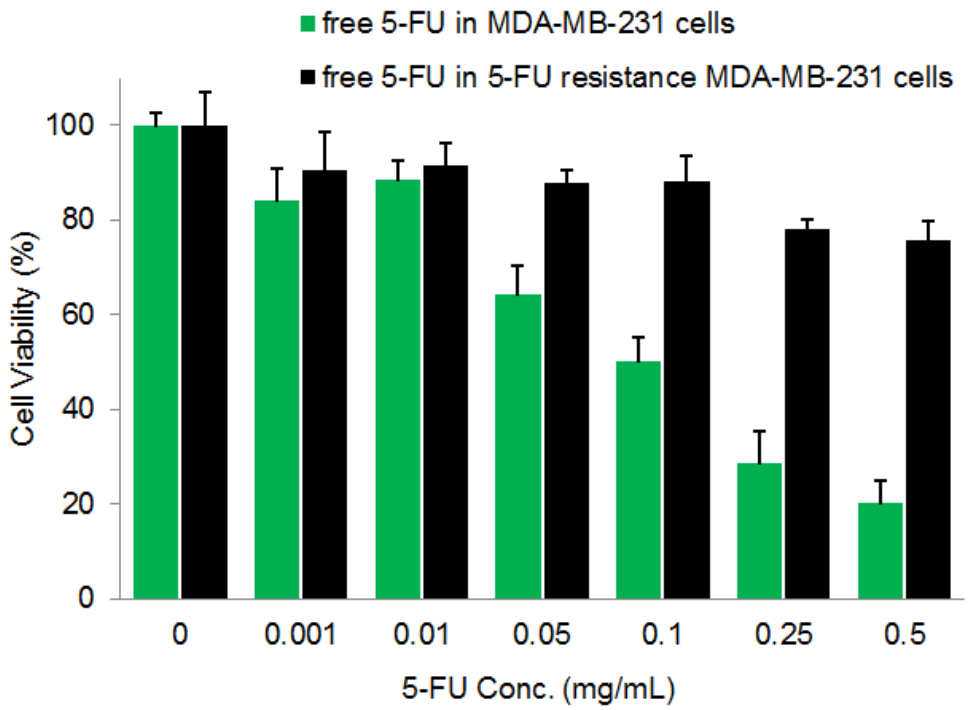

Figure S8. MTT assay for a resistant breast cancer cell line MDA-MB-231 after continuous exposure to drug, when compared to parental cancer cells. The resistant breast cancer cell line MDA-MB-231 was obtained by continuous culture of parental MDA-MB-231 cells in 5-FU and maintained with 5-FU at a dose of 0.05 mg/mL.

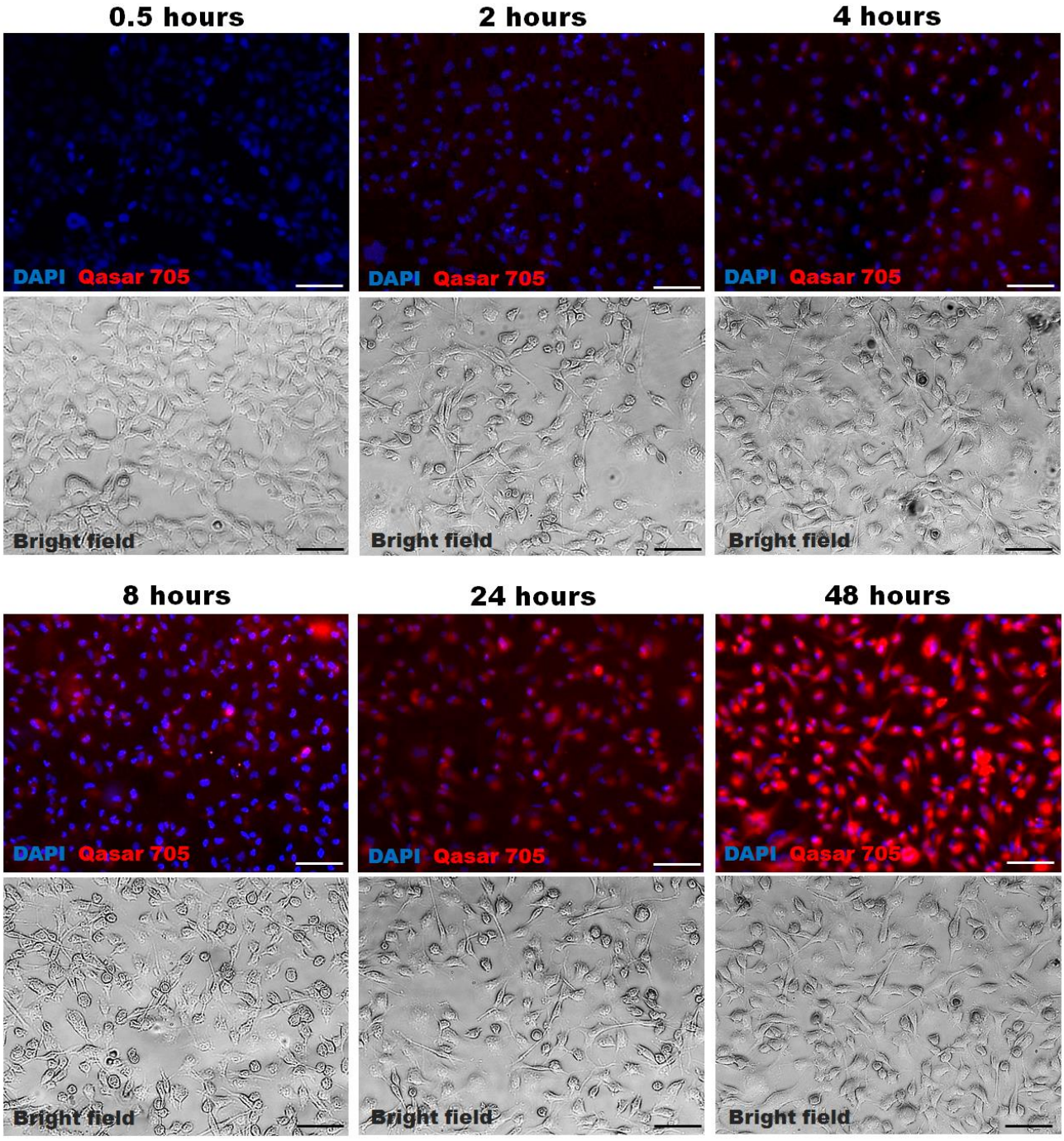

Figure S9. Nanobeacons cellular uptake for different time points (0.5 to 48 hours). Scale bars, 50 μm.

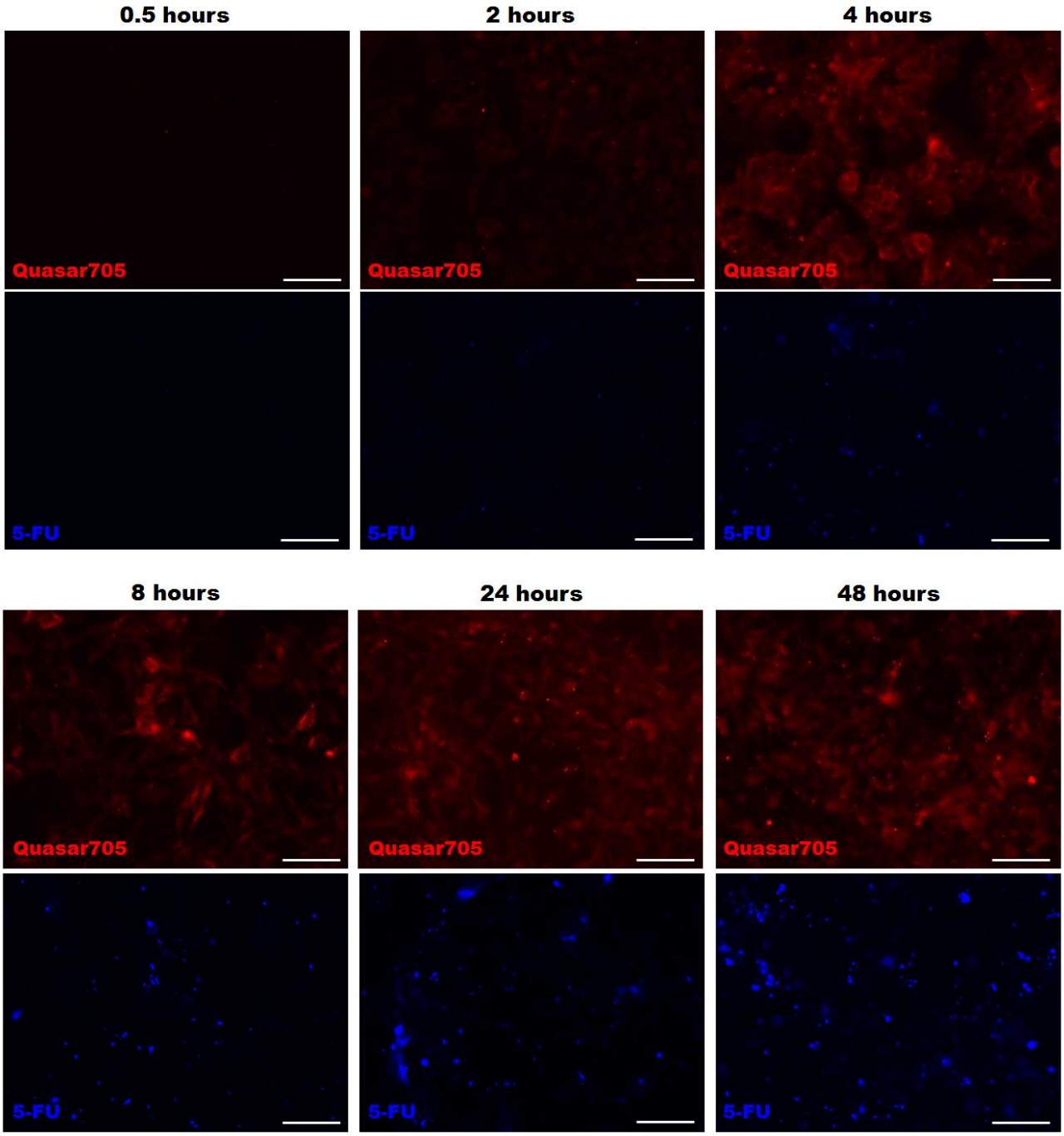

Figure S10. Nanobeacons cellular uptake and detection associated with drug (5-FU) release signal for different time points (0.5 to 48 hours). Scale bars, 20 μm.

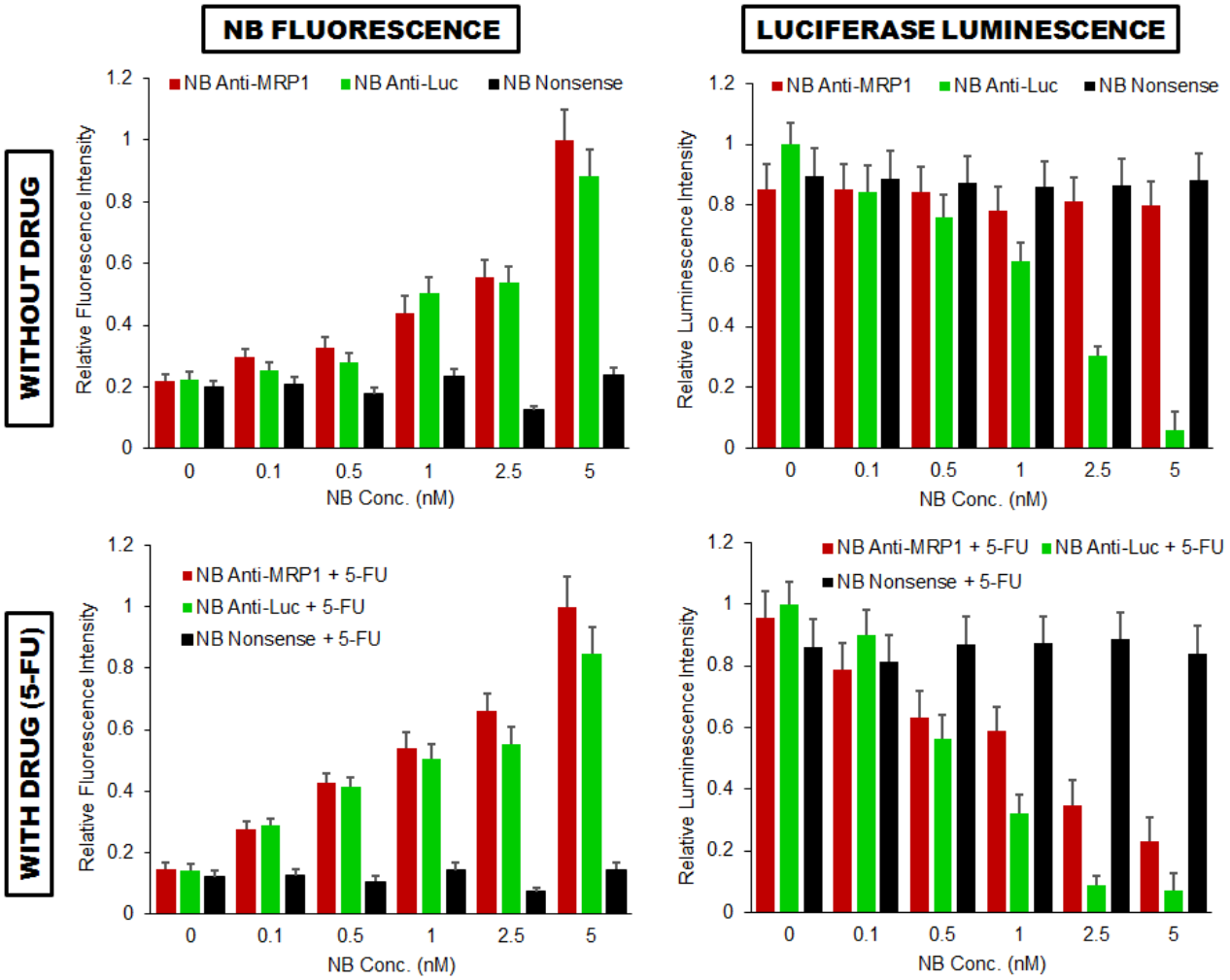

Figure S11. Quantification of luminescence and fluorescence signals from IVIS images (see **Figure 3A** of the main manuscript) of resistant MDA-MB-231 cells incubated with increasing amounts (0.1 to 5 nM) of dark-gold nanobeacons without and with 5-FU. NB stands for nanobeacon.

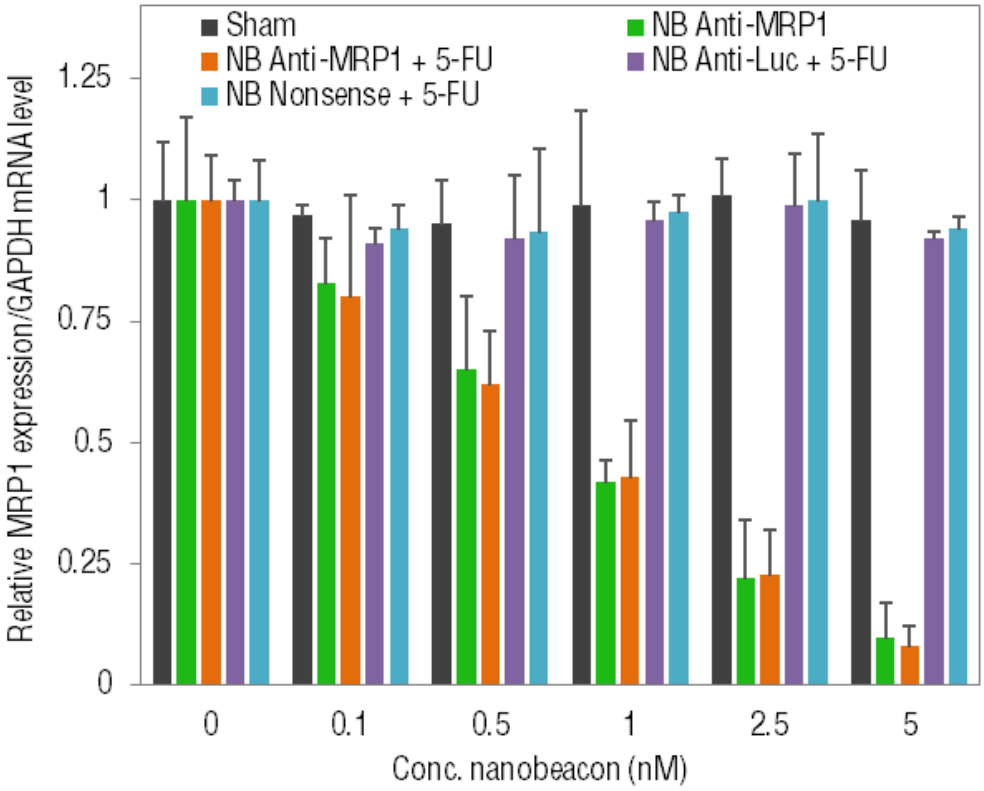

Figure S12. The silencing effect was expressed as a concentration-dependent decrease in MRP1 relative expression. Only nanobeacons anti-MRP1 loaded with 5-FU showed potent silencing with an ED50 around 1 nM for 48 hours of incubation. Data points represent group mean ± SD (n = 3). GAPDH was used as the reference gene.

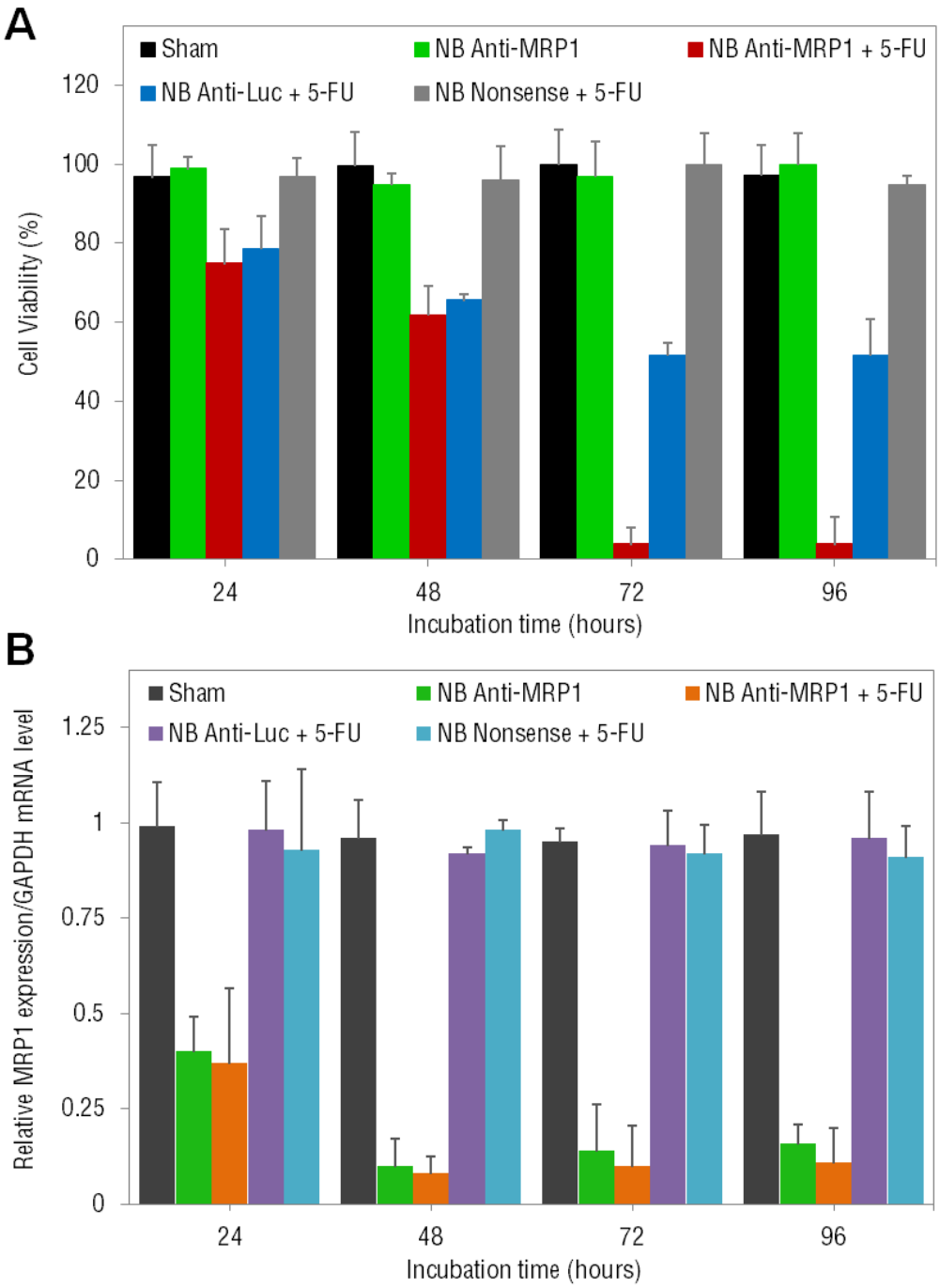

Figure S13. (**A**) Kinetics for the effect of 5-FU release in cell viability via MTT assay for 24, 48, 72 and 96 hours using 5 nM (the same concentration for *in vitro* and *in vivo* studies) of nanobeacons loaded with 5-FU. (B) Kinetics for MRP1 expression using the same nanobeacons at 5 nM, for 24, 48, 72 and 96 hours. GAPDH was used as the reference gene. Data points represent group mean ± SD (n = 3).

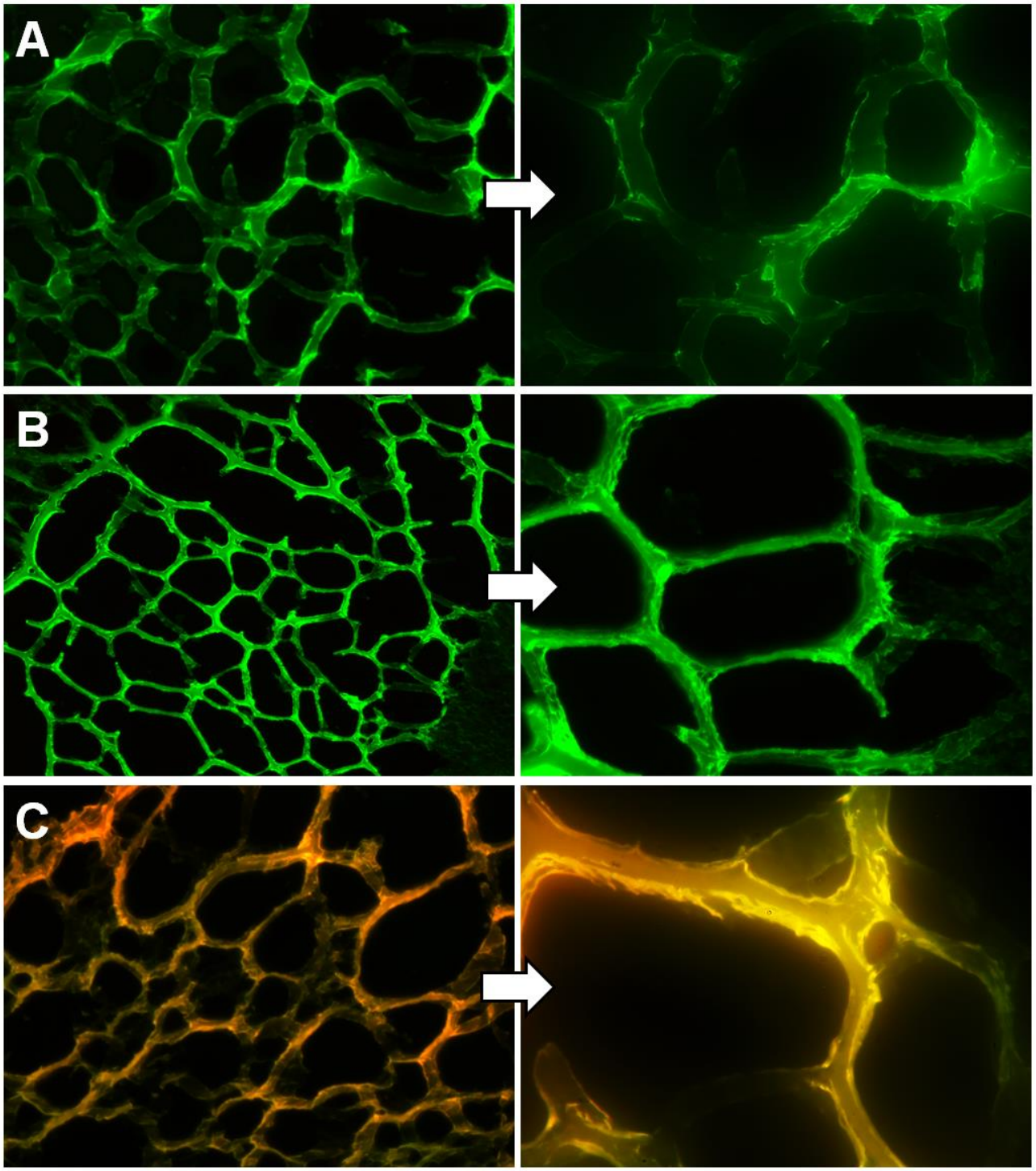

Figure S14. (**A**) Cryosection of dendrimer:dextran adhesive hydrogel (12 um thickness) where dextran aldehyde was tagged with fluorescein. (**B**) Cryosection of nanobeacon-doped dendrimer:dextran scaffold without the incubation of any target. (**C**) Cryosection of nanobeacon-doped dendrimer:dextran scaffold previously incubated with a complementary target. Nanobeacons (red) are uniformly distributed in the hydrogel scaffold (green).

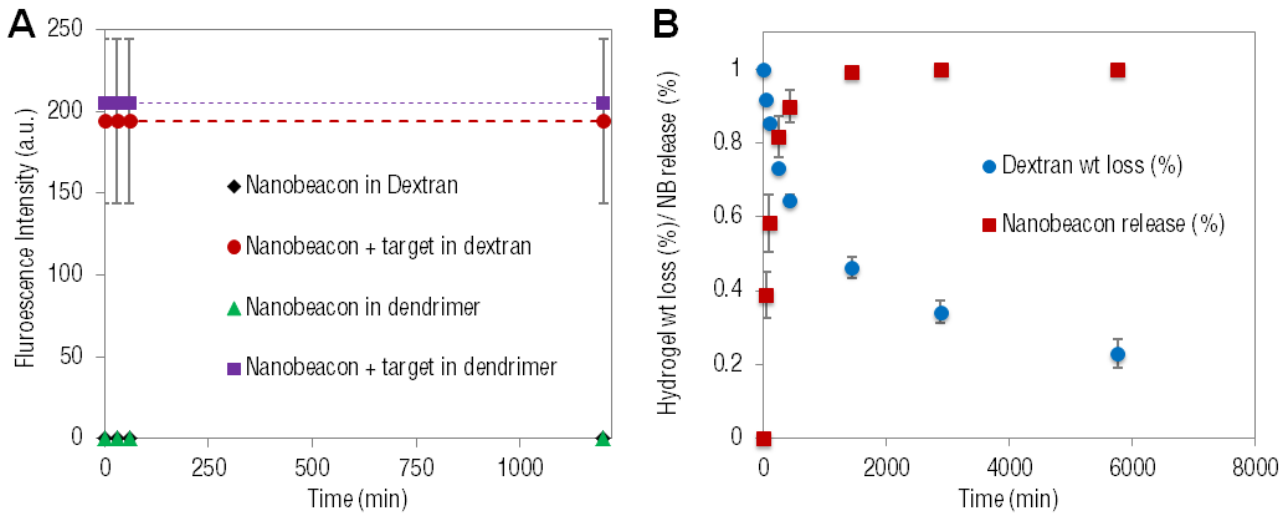

Figure S15. (**A**) Stability assay for nanobeacons with and without target in the presence of dextran 5% and dendrimer 12.5% components during 24 hours. (**B**) Release profile of nanobeacons from the dendrimer:dextran scaffold during 96 hours. An almost complete release in the first 24 hours under physiological conditions *in vitro* was observed (pH 7.4 and 37ºC).

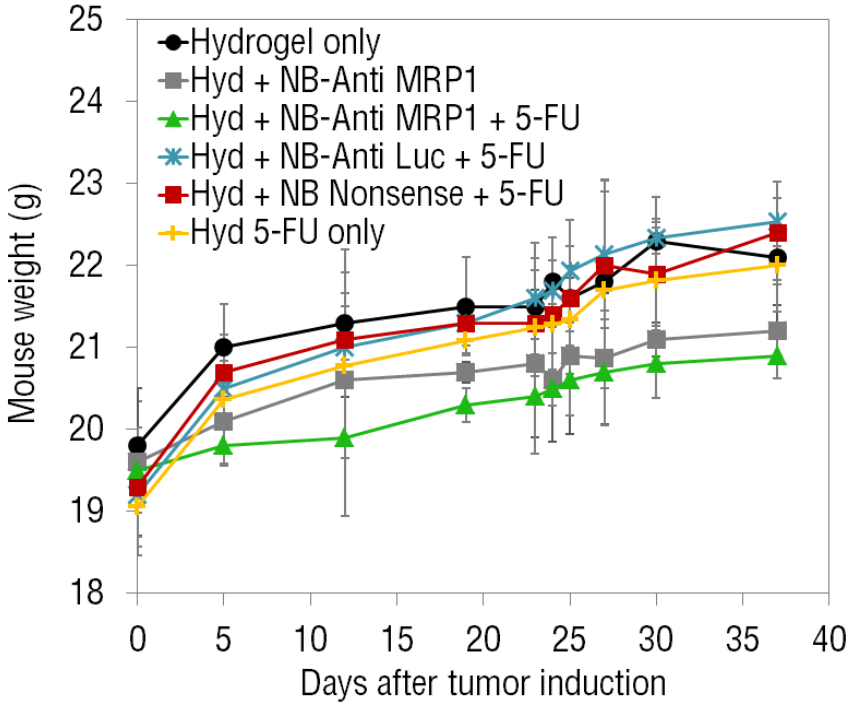

Figure S16. The safety of hydrogel doped with nanobeacons was confirmed by monitoring body weight as a proxy for tolerability. Body weight assessment was performed on all the animal groups during 37 days after breast cancer cells injection. Body weight depicted as the mean of each treatment group. No decrease or changes in body weight were found for all treatment mice groups (n = 5).

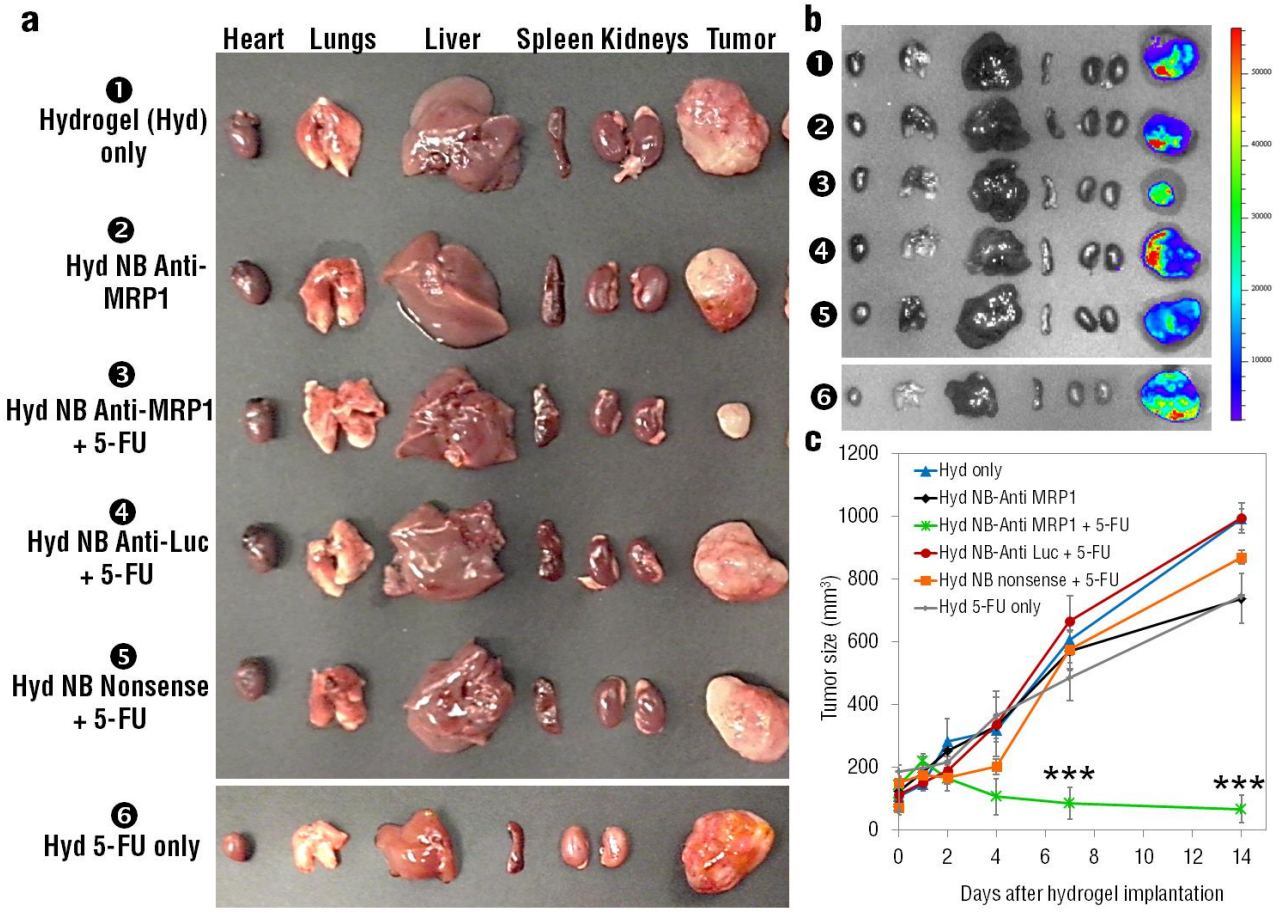

Figure S17. Representative photographs (**a**) and luminescence images (**b**) of whole body organs and resected tumors in mice (n = 5) treated with nanobeacons, corroborating the results of tumor size reduction after hydrogel implantation, measured by (**c**).

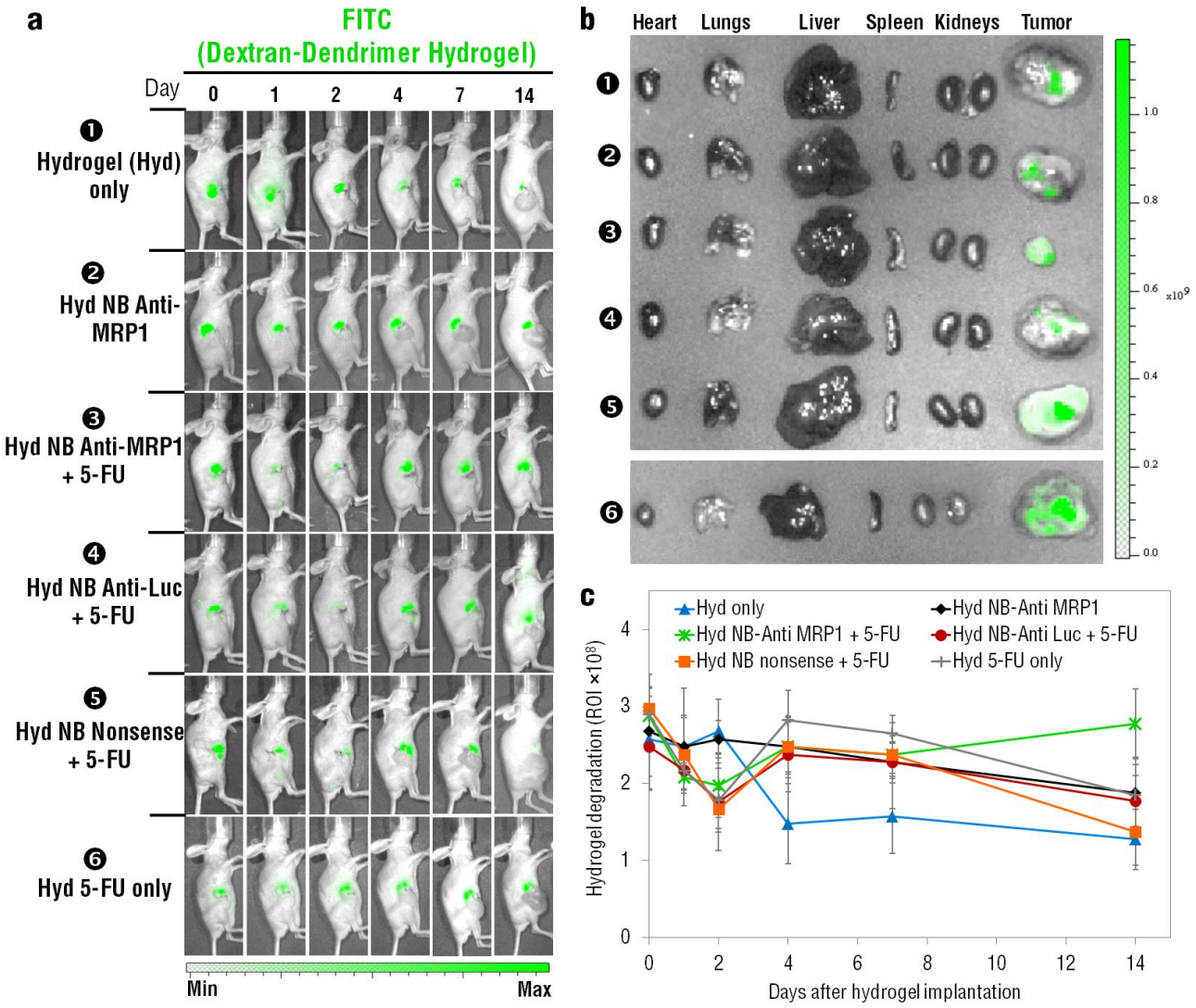

Figure S18. *In vivo* hydrogel degradation monitored by FITC intensity following implantation in mice (n = 5) (**a**) and in *ex vivo* organs (**b**), showing the highest signals during the first 2 days were hydrogel degrades rapidly, and continues to degrade about 45-50% after 14 days (**c**).

Aditional references

S1. Conde, J. *et al.* (2012) Design of multifunctional gold nanoparticles for in vitro and in vivo gene silencing. *ACS Nano.* **6**, 8316-8324.

S2. Conde, J., Rosa, J., de la Fuente, J.M., Baptista, P.V. (2013) Gold-nanobeacons for simultaneous gene specific silencing and intracellular tracking of the silencing events. *Biomaterials* **34**, 2516-2523.

S3. Conde, J., de la Fuente, J.M., Baptista, P.V. (2010) In vitro transcription and translation inhibition via DNA functionalized gold nanoparticles. *Nanotechnology.* **21**, 505101.

S4. Conde, J., de la Fuente, J.M., Baptista, P.V. (2010) RNA quantification using gold nanoprobes - application to cancer diagnostics. *J. Nanobiotechnology.* **8**, 5.

S5. Zadeh, J.N., Steenberg, C.D., Bois, J.S., Wolfe, B.R., Pierce, M.B., Khan, A.R., Dirks, R.M., Pierce, N.A. (2011) NUPACK: Analysis and design of nucleic acid systems. *J. Comput. Chem.* **32**, 170-173.